Preprint Volume, 26th Conf. on Radar Meteorology, Norman, OK, AMS, May 24-28, 1993, 447-450.

Three-dimensional validation at TRMM ground truth sites: Some early results from Darwin, Australia

by

Matthias Steiner and Robert A. Houze, Jr.

Department of Atmospheric Sciences, AK-40,
University of Washington
Seattle, WA 98195

1. Introduction

The Tropical Rainfall Measuring Mission (TRMM) has been designed to obtain quantitative precipitation measurements from space within the tropics on a global scale (Simpson et al. 1988). The ultimate goal is to evaluate the four-dimensional structure of latent heating in the tropical atmosphere. An important part of this undertaking is the surface verification, or Ground Truth Program. This ground-based validation will build upon measurements obtained from a number of sites within the tropics.

TRMM ground truth sites have been chosen to represent the various regimes of tropical rainfall. Each site will be equipped with a weather radar, a surrounding network of raingauges, and disdrometer(s). Data at a few sites have already been collected for several years. Standards of achieving representative precipitation climatologies from these data and methods for combining and integrating the various monthly data products must be developed to provide the four-dimensional heating required to validate and assess the upcoming TRMM satellite measurements. It is vital to the TRMM Ground Truth Program to have an efficient model for extracting and combining the key information from the data set for a given site.

We have undertaken a pilot study to derive a three-dimensional surface verification data set from a typical month of data, integrating all the available data products collected at a particular station. The goal is to determine, with the minimum amount of data processing, not only the amount of precipitation, but also its subdivision into convective and nonconvective (i.e., stratiform) components and its vertical structure. For this pilot study we use the data obtained at Darwin, Australia during February 1988. We present methods for distinguishing convective and nonconvective regions, establishing the Z-R relations that apply to each region, and determining the fractions of convective and nonconvective rain that contribute to the total precipitation. We will further investigate the sensitivity of the results to the spatial resolution of the radar data.

2. February 1988: Data overview

a. Meteorological overview

February 1988 was a fairly typical month. The precipitation totaled about 20% less than the long-term average (NOAA 1988). The mean areal rainfall determined by the raingauge network totaled 225 mm. The daily rainfall amounts exhibit a large variability (Fig. 1): seven days had rainfall amounts larger than 10 mm, accounting for about 70% of the monthly total rainfall. Ten days exhibited less than 1 mm.

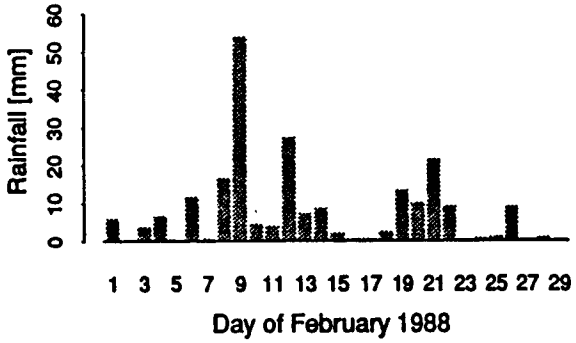

Fig. 1. Daily areal mean rainfall amounts for February 1988, based on the Darwin raingauge network.

b. Available data

During February 1988 the Darwin ground truth site was equipped with the NOAA/TOGA Doppler radar (C-band) and a mesoscale network of 23 recording raingauges. Although the instrumentation of the Darwin site includes a disdrometer of the Joss-Waldvogel (1967) type, no disdrometer data were available for this particular month.

Six different radar-scan strategies (base scan, different volume and vertical scans) were used during February 1988 (see Keenan et al. 1988). For the present study, only the 12 elevation volume scans were investigated to establish the three-dimensional precipitation climatology for this month. That type of scan was performed about every 15 min during intensive observation periods and less frequently otherwise. About 1800 volume scans were thus obtained for February 1988.

3. February 1988: Data analysis

a. General radar data processing

We selected specific radar volumes for our analysis. These radar volume scans are manually edited with respect to identification and removal of second-trip echoes, ground clutter, and anomalous propagation. After the radar data have been edited, they are bilinearly interpolated into a Cartesian grid using two different grid resolutions: one having a 4-km horizontal and 3-km vertical resolution, and the other a 2-km horizontal and a 1.5-km vertical resolution. These processing steps are performed by means of standard NCAR radar data processing software (RDSS, SPRINT).

Our analysis for February 1988 is based on the radar volume scans closest to 0330 and 1530 h local time (= GMT + 9 1/2 h). Six out of the 58 possible radar volumes had to be withdrawn from further processing because of the quality of the recorded raw data. The data analysis is thus

based on two times a day. This time resolution corresponds roughly to that of the TRMM satellite.

The areal mean and monthly averaged radar reflectivities, stratified by their distance from the radar site, indicate no significant range dependency out to the maximum range considered (about 170 km). There is generally good agreement between the data at both 2 and 4-km horizontal resolution. However, within the first 10 km the higher resolution grid reflectivities tend to be ~ 7 dBZ higher than the 4-km resolution data. No range corrections of any type have been applied to the radar data.

b. Separating convective from nonconvective precipitation

An important ground-truth objective is the separation of precipitation echoes into convective and nonconvective elements. We use a modification of the technique applied by Churchill and Houze (1984; hereafter CH84) to separate the radar echo pattern into convective and nonconvective parts. CH84 first converted the low-level horizontal pattern of radar reflectivity to a field of rain rate by applying a Z-R relation, of the form

$$Z = A R^b \qquad (1)$$

where Z is the radar reflectivity and R the rainfall intensity. CH84 then defined the center of a convective cell to be a maximum of rain rate that either exceeds a given threshold rain rate or exceeds the background rain rate by a factor of two or more. The limitation of their technique is that a single Z-R relation is applied to all of the radar echo. Therefore, this procedure does not allow separate Z-R relationships to be applied to the convective and nonconvective precipitation since the separation is done after converting reflectivities into rainfall intensities. However, Joss and Waldvogel (1970) and Joss et al. (1970) have shown that application of different Z-R relations to the convective and stratiform portions of a precipitation area can substantially improve the overall estimation of rainfall. Short et al. (1992) came to a similar conclusion; namely, that convective and nonconvective parts of tropical squall lines are characterized by two quite different Z-R relationships.

We modified the CH84 procedure by applying a separation algorithm to the reflectivity field at the 3-km altitude level before any reflectivities are converted to rain rate. Following the general idea of the CH84 scheme, we assume that convective cells are centered on any reflectivity that exceeds a certain threshold (here taken to be 40 dBZ) and any other reflectivity that exceeds the background radar reflectivity by 4.5 dBZ, where the background area is a region of defined size surrounding the center of the cell (Table 1). The 4.5 dBZ difference corresponds roughly to a factor of two difference in rain rate [if the exponent b in (1) is assumed to be 1.5]. Once an echo at a grid point is designated as the center (or core) of a convective cell by one of the above criteria, an area of assumed size surrounding the core is also said to be convective (Table 1). Thus, any grid points not designated as convective are considered to be nonconvective. After the whole echo region is divided into convective and nonconvective areas, separate Z-R relations are determined and applied to the convective and nonconvective areas (see Section 3c).

Applications of the modified CH84 technique to the February 1988 Darwin data indicates that the mean percentage of the total radar-echo area at 3-km altitude covered by convective precipitation is about 45% if the 2-km resolution grid is used, but it is only 31% for the 4-km resolution data. The higher resolution grid thus shows 14% more convective echoes, even though the convective area around a given core is deemed to be smaller than the one used for the 4-km resolution data (Table 1). The increased convective area is the result of the much more detailed

TABLE 1. Background area and convective ring around convective cores for the two different grid resolutions used in this study. The background corresponds to a 5 x 5 and 11 x 11 grid point area for the 4-km and 2-km horizontal resolution grid respectively, while the convective ring is based on one ring of grid points around the core point (convective area = 3 x 3 grid points) for the lower and two rings of grid points (5 x 5) for the higher resolution data.

Horizontal grid resolution	Background area	convective ring around core
4 km (=CH84)	400 km^2	144 km^2
2 km	484 km^2	100 km^2

structures reflected by the higher-resolution reflectivity fields. The frequency distribution of the area percentages of convective echoes for February 1988 shows much larger contributions from higher percentages of convective area coverage for the 2-km than the 4-km resolution data (Fig. 2). The relative maximum around 45% in the distribution of the lower resolution data is shifted toward larger values with increasing grid resolution. The frequency distribution of the higher resolution data exhibits a much broader peak between about 50-80% of the area coverage by convective precipitation.

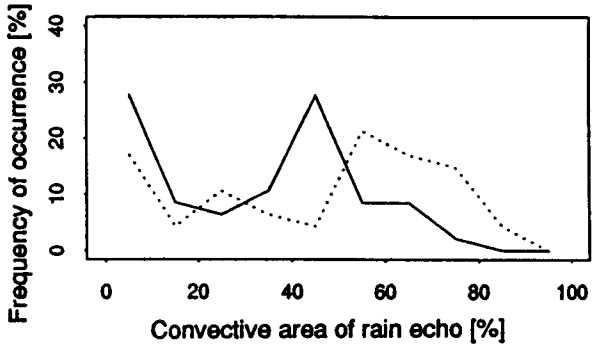

Fig. 2. Distribution of the percentage of the area covered by convective precipitation echoes. The solid line represents the 4-km grid resolution data, while the dashed line shows the results of the 2-km gridded data.

The increase of the convective area coverage to higher percentages for the higher resolution grid data is associated with a relative increase of the number of grid points with convective reflectivities in the range of 5-40 dBZ. The normalized frequency distributions of convective and nonconvective reflectivities, however, are almost identical for both grid resolutions (Fig. 3). Compared to the nonconvective distribution, the convective reflectivities are in the 15-20 dBZ range, while the distribution of the convective radar-echo values is somewhat broader than the nonconvective and peaks at 20-30 dBZ. Future work will compare the current method of separating convective from nonconvective precipitation with the principal mode analysis performed by Bell and Ravipati (1992).

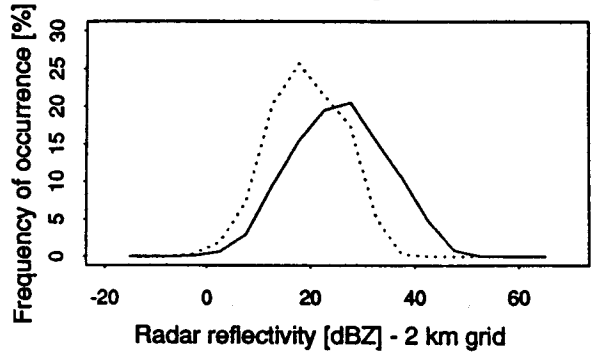

Fig. 3. Normalized frequency distributions of the radar reflectivities from convective (solid line) and nonconvective (dashed line) precipitation, based on the 2-km horizontal resolution gridded data.

The heating of the atmosphere is strongly associated with the vertical precipitation structure (Houze 1989), which in turn is associated with whether the precipitation is convective or nonconvective. It is important therefore not only to separate convective from nonconvective precipitation but also to address their typical vertical structures. Figure 4 shows the area and time-averaged mean vertical reflectivity profiles for February 1988 at the Darwin ground truth site. The profiles for the convective and nonconvective precipitation are obtained by first horizontally averaging the respective grid volumes identified as convective and nonconvective and then averaging all of the corresponding profiles in time. The vertical reflectivity profiles are basically the same for both grid resolutions used in this study, except that the higher resolution profiles show more details in the vertical structure. The bright band, a primary signature of nonconvective precipitation, is well resolved by the higher resolution grid data. This result is a good indicator of the quality of the applied separation technique. The mean convective and nonconvective vertical reflectivity profiles are very similar, though the convective profile is shifted by about 5-10 dBZ toward higher intensities. The averaged nonconvective profile shows an increase in the intensity at upper levels, which may in some way have been produced by the large anvil clouds of tropical precipitation systems. Since the coherent structure in these vertical profiles appears even though they represent an average in space and time, a mixture of vertical structures over ocean and land, and different life cycle stages of precipitation systems, we conclude that the separation technique must be generally reliable, but that it is better applied with 2-km horizontal (and 1.5-km vertical) resolution than 4-km horizontal (3-km vertical) resolution.

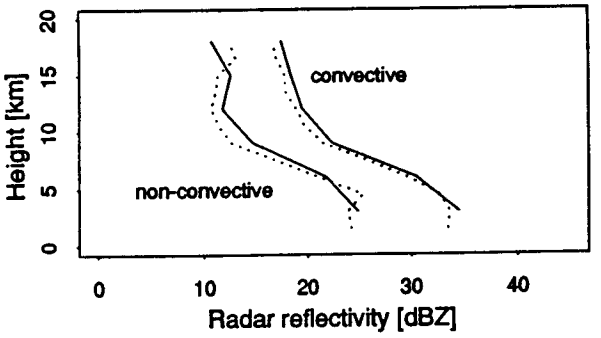

Fig. 4. Area and time averaged mean vertical reflectivity profiles of convective and nonconvective precipitation for February 1988 at the Darwin TRMM ground truth site. The solid line represents the 4-km grid resolution data, while the dashed line shows the results of the 2-km gridded data.

c. Calibrating the radar-based rainfall estimates

To improve the accuracy of the conversion of radar reflectivities into rainfall intensities we apply different *Z-R* relations to the convective and nonconvective precipitation areas identified by the separation technique. The following procedure has been developed to adjust the factors *A* and *b* in (1) to convective and nonconvective precipitation observed during February 1988 at the Darwin ground truth site. A 15-min window starting at the radar observation time is applied to the raingauge data to determine the contemporaneous rainfall intensity at each gauge site. As a result, a number of radar reflectivity (at the raingauge site)/ rainfall intensity (raingauge-base) pairs are obtained which corresponds to the number of radar volume scans times the number of raingauge sites. The ensemble of these pairs is then subdivided into convective and nonconvective pairs according to the radar-based identification. The convective and nonconvective *Z-R* relationships are determined for each subset of data pairs (where both raingauge and radar indicate simultaneously rain or no-rain) by adjusting the factor *A* such that the radar-derived mean rainfall intensity matches the raingauge-base value,

$$A = \left[\Sigma Z_i^{1/b} / \Sigma R_i\right]^b \qquad (2)$$

while setting the factor *b* to 1.5, the value used above for the separation of convective and nonconvective precipitation. The justification for this can be found in the results of Joss et al. (1970) who suggested that *b* is often close to 1.5 in drizzle, stratiform precipitation, and thunderstorm rain, while *A* may change significantly from one precipitation type to another. Because of some data pairs for which the radar indicates rain while the raingauge does not and vice versa (Table 2), both the convective and the nonconvective factors *A* have to be multiplied by the same correction factor to ensure that the radar-based mean areal rainfall at the raingauge sites matches the raingauge-based estimate. Using the 4-km horizontal resolution radar reflectivity data, the resulting relationships are

$$Z = 50\,R^{1.5} \qquad (3)$$

for the convective and

$$Z = 115\,R^{1.5} \qquad (4)$$

for the nonconvective precipitation during February 1988 at the Darwin ground truth site.

Other ways exist to determine the *Z-R* relationships including, for example, a linear regression analysis of the radar reflectivity/rainfall intensity pairs to determine the factors *A* and *b*, and the different probability-matching methods described by Calheiros and Zawadzki (1987), Atlas et al. (1989), or Rosenfeld et al. (1992). The former technique is not appropriate here because of the relatively low number of data pairs in the subsets. The probability-matching method is an interesting, independent approach which should be explored in future work. Future studies should also derive *Z-R* relationships based on raindrop spectra measurements.

Total areal mean rainfall estimates for an area 240 km x 240 km surrounding the Darwin radar site for February 1988 are summarized in Table 2. The twice daily item resolution used here evidently does not yield an accurate areal rainfall total for the month, as indicated by the difference in the continuous raingauge estimate and the one based on the radar observation times. The radar estimate at the raingauge sites is tuned to be the same as the corresponding raingauge accumulation, as described earlier. There is a significant difference in the rain amount estimates based on the radar values at the raingauge site (land-based only) and the areal mean rainfall determined by considering the fully available radar information, which also includes data over the ocean.

TABLE 2 Different areal mean rainfall estimates for February 1988 at Darwin, Australia. The radar estimates are based on the 4-km horizontal resolution data and two volumes per day.

Raingauge	(continuous)	225 mm
Raingauge	(15 min interval at radar times)	336 mm
Radar	(estimate at raingauge sites)	336 mm
Radar	(full area consideration)	254 mm

Figure 5 depicts the frequency distribution of the convective contribution to the areal rainfall amount of the different radar volumes investigated in the present study. Based on the two radar volumes analyzed per day, Fig. 5 shows an enhanced frequency of occurrence of both small and especially of large contributions of convective rainfall to the total areal amount. The reasons for this bimodal distribution are not yet clear. However, they may be related to the diurnal cycle and/or differences between land and ocean, as demonstrated by many other studies (e.g., Houze et al. 1981; Williams and Houze 1987; Keenan et al. 1988). Again, there are differences in the results obtained by the two different grid resolutions which are in concert with our foregoing findings about the area covered by convective precipitation echoes. The results that are based on the 4-km resolution grid indicate that on average about 57% of the total rain observed during February 1988 at the Darwin ground truth site was contributed by convective precipitation. This is in good agreement with earlier findings from GATE and MONEX for other tropical regimes (e.g., CH84). The higher resolution data, on the other hand, indicate with 69% a somewhat larger contribution from convective rainfall.

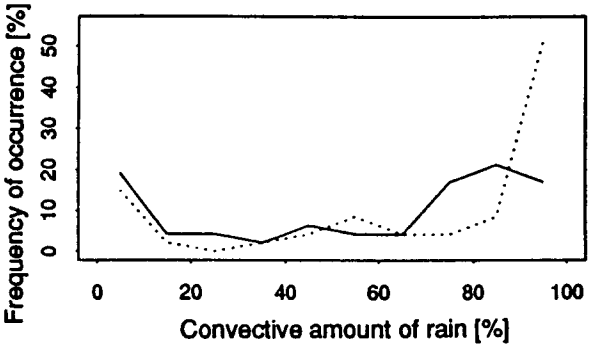

Fig. 5. Distribution of the percentage of the areal rainfall contributed by convective precipitation. The solid line represents the 4-km grid resolution data, while the dashed line shows the results of the 2-km gridded data.

4. Summary and outlook for future analysis

Techniques of representing ground truth for TRMM from a single tropical site are tested by examining two volume scans per day taken by the Darwin, Australia C-band Doppler radar during February 1988. In this study, we have developed methods for separating the convective and nonconvective components of the precipitation, and for representing the vertical structure of the radar reflectivity. In particular, we have sought to identify the spatial resolution required to represent these features of the three-dimensional precipitation structure.

The technique used to separate the convective from the nonconvective precipitation is applied to the radar reflectivity field before any *Z-R* relation is applied to convert the reflectivity to rain rate. This order of analysis allows for the application of a separate *Z-R* conversion to the convective and nonconvective precipitation areas.

The vertical structure of the radar echo is determined at low (4-km horizontal, 3-km vertical) and high (2-km horizontal, 1.5-km vertical) resolution. The higher resolution was required in order for the bright band to appear in the averaged, nonconvective vertical profile.

Coincident and contemporaneous radar and raingauge data were used to derive separate *Z-R* relations for the convective and nonconvective precipitation. Application of these relations to the convective and nonconvective areas of precipitation determined by the scheme described above showed that the convective precipitation areas (31-45% averaged echo area coverage) accounted for 57-69% of the total rain. The lower estimate was obtained from the 4-km horizontal resolution data, while the higher estimate was obtained from the 2-km resolution data.

The presented data analysis procedures will be extended in the near future to include consideration of ocean-land differences and the corresponding diurnal cycles, which requires higher time resolution. Furthermore, the technique for distinguishing convective from nonconvective precipitation should be compared with the principal mode technique (Bell and Ravipati 1992) and the determination of the areal rainfall using probability-matching methods (Calheiros and Zawadzki 1987; Atlas et al. 1990; Rosenfeld et al. 1992). The Doppler radial velocity estimates for those times when precipitation fully surrounds the radar site will be analyzed to determine the vertical profile of horizontal wind divergence, which is related closely to the vertical profile of heating in tropical precipitation (Mapes and Houze 1992, 1993). Finally, an important experiment to be carried out in the future is to rerun the different analyses described herein on the basis of the unedited radar data in order to explore the influence of ground clutter, second-trip echoes, and anomalous propagation on the derived precipitation climatologies.

Acknowledgments: We are grateful to Otto Thiele, Dennis Flanigan, and David Wolff for their effort in providing the Darwin radar and raingauge data. Sandra Yuter is acknowledged for her computational support and consulting and Mark Albright also provided assistance. G. C. Gudmundson edited the manuscript and K. M. Dewar did the layout. This work is supported by NASA grant NAG 5-1599.

References

Atlas, D., D. A. Short, and D. Rosenfeld, 1989. *Preprints, 24th Conference on Radar Meteorology*, Tallahassee, Florida, Amer. Meteor. Soc., 666-671.

Atlas, D., D. Rosenfeld, and D. B. Wolff, 1990. *J. Appl. Meteor.*, **29**, 1120-1135.

Bell, T. L., and S. Ravipati, 1992. *Proceedings, Fifth International Meeting on Statistical Climatology*, Toronto, Canada, Amer. Meteor. Soc., 225-228.

Calheiros, R. V., and I. Zawadzki, 1987. *J. Clim. Appl. Meteor.*, **26**, 118-132.

Churchill, D. D., and R. A. Houze, Jr., 1984. *J. Atmos. Sci.*, 41, 933-960.

Houze, R. A., Jr., 1989. *Quart. J. Royal Meteor. Soc.*, **115**, 425-461.

Houze, R. A., Jr., S. G. Geotis, F. D. Marks, Jr., and A. K. West, 1981. *Mon. Wea. Rev.*, **109**, 1595-1614.

Joss, J., and A. Waldvogel, 1967. *Pure Appl. Geophys.*, **68**, 240-246.

Joss, J., and A. Waldvogel, 1970. *Proceedings, 14th Radar Meteorology Conference*, Tucson, Arizona, Amer. Meteor. Soc., 237-238.

Joss, J., K. Schram, J. C. Thams and A. Waldvogel, 1970. Wiss. Mitteilung Nr. 63 der Eidgen, Kommission zum Studium der Hagelbildung und der Hagelabwehr, ETH Zürich, 38 pp.

Keenan, T. D., G. J. Holland, M. J. Manton, and J. Simpson, 1988. *Aust. Met. Mag.*, **36**, 81-90.

Mapes, B. E., and R. A. Houze, Jr., 1992. *Quart. J. Royal Meteor. Soc.*, **118**, 927-963.

Mapes, B. E., and R. A. Houze, Jr., 1993. Part II: Vertical structure. *Quart. J. Royal Meteor. Soc.* (in press).

NOAA, 1988. **41**, No. 2, National Climatic Data Center, Asheville, North Carolina.

Rosenfeld, D., D. B. Wolff, and E. Amitai, 1992. The window probability-matching method for rainfall measurements with radar. Submitted, *J. Appl. Meteor.*

Short, D. A., T. Kozu, K. Nakamura and T. D. Keenan, 1992. On stratiform rain in the tropics. Submitted, *J. Meteor. Soc. Japan.*

Simpson, J., R. F. Adler and G. R. North, 1988. *Bull Amer. Meteor. Soc.*, **69**, 278-295.

Williams, M., and R. A. Houze, Jr., 1987. *Mon. Wea. Rev.*, **115**, 505-519.